JACS
JOURNAL OF THE AMERICAN CHEMICAL SOCIETY
Article
pubs.acs.org/JACS

Dioxygen Activation and Catalytic Reduction to Hydrogen Peroxide by a Thiolate-Bridged Dimanganese(II) Complex with a Pendant Thiol

Marcello Gennari,[*,†] Deborah Brazzolotto,[†] Jacques Pécaut,[‡,⊥] Mickael V. Cherrier,[§,∥,#,∇] Christopher J. Pollock,[⊗,□] Serena DeBeer,[⊗,×] Marius Retegan,[⊗] Dimitrios A. Pantazis,[⊗] Frank Neese,[⊗] Mathieu Rouzières,[¶,▲] Rodolphe Clérac,[¶,▲] and Carole Duboc*[,†]

[†]CNRS UMR 5250, DCM, Université Grenoble Alpes, F-38000 Grenoble, France
[‡]INAC-SCIB, Université Grenoble Alpes, F-38000 Grenoble, France
[⊥]Reconnaissance Ionique et Chimie de Coordination, CEA, INAC-SCIB, F-38000 Grenoble, France
[§]Metalloproteins Unit, Institut de Biologie Structurale Jean-Pierre Ebel, CEA, CNRS UMR 5075, Université Grenoble Alpes, 41 rue Horowitz, 38027 Grenoble Cedex 1, France
[∥]Université de Lyon, F-69622 Lyon, France
[#]Université Claude Bernard Lyon 1, F-69622 Villeurbanne, France
[∇]CNRS, UMR 5086 Bases Moléculaires et Structurales de Systèmes Infectieux, Institut de Biologie et Chimie des Protéines, 7 Passage du Vercors, F-69367 Lyon, France
[⊗]Max-Planck-Institut für Chemische Energie Konversion, Stiftstrasse 34-36, D-45470 Mülheim an der Ruhr, Germany
[×]Department of Chemistry and Chemical Biology, Cornell University, Ithaca, New York 14853, United States
[¶]CNRS, CRPP, UPR 8641, F-33600 Pessac, France
[▲]CRPP, UPR 8641, Université Bordeaux, F-33600 Pessac, France

Supporting Information

ABSTRACT: Herein, we describe an uncommon example of a manganese−thiolate complex, which is capable of activating dioxygen and catalyzing its two-electron reduction to generate H_2O_2. The structurally characterized dimercapto-bridged Mn^{II} dimer $[Mn^{II}_2(LS)(LSH)]ClO_4$ (**Mn^{II}_2SH**) is formed by reaction of the LS ligand (2,2′-(2,2′-bipyridine-6,6′-diyl)bis-(1,1-diphenylethanethiolate)) with Mn^{II}. The unusual presence of a pendant thiol group bound to one Mn^{II} ion in **Mn^{II}_2SH** is evidenced both in the solid state and in solution. The **Mn^{II}_2SH** complex reacts with dioxygen in CH_3CN, leading to the formation of a rare mono-μ-hydroxo dinuclear Mn^{III} complex, $[(Mn^{III}_2(LS)_2(OH)]ClO_4$ (**Mn^{III}_2OH**), which has also been structurally characterized. When **Mn^{II}_2SH** reacts with O_2 in the presence of a proton source, 2,6-lutidinium tetrafluoroborate (up to 50 equiv), the formation of a new Mn species is observed, assigned to a bis-μ-thiolato dinuclear Mn^{III} complex with two terminal thiolate groups (**Mn^{III}_2**), with the concomitant production of H_2O_2 up to ∼40% vs **Mn^{II}_2SH**. The addition of a catalytic amount of **Mn^{II}_2SH** to an air-saturated solution of Me_nFc (n = 8 or 10) and 2,6-lutidinium tetrafluoroborate results in the quantitative and efficient oxidation of Me_nFc by O_2 to afford the respective ferrocenium derivatives (Me_nFc^+, with n = 8 or 10). Hydrogen peroxide is mainly produced during the catalytic reduction of dioxygen with 80−84% selectivity, making the **Mn^{II}_2SH** complex a rare Mn-based active catalyst for two-electron O_2 reduction.

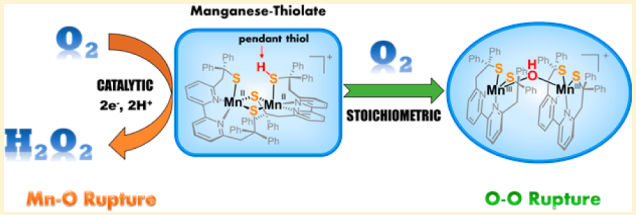

1. INTRODUCTION

Activation of dioxygen represents a critical step in numerous fundamental biological and industrial processes.[1] This is a prerequisite for O_2-promoted selective oxidation and oxygenation of organic substrates,[2,3] and for proton-assisted catalytic reduction of O_2. The four-electron O_2 reduction process plays an essential role in sustaining life (aerobic respiration)[4,5] and generating electrical energy (in fuel cells).[6,7] On the other hand, two-electron O_2 reduction generates hydrogen peroxide, a versatile and environmentally benign oxidizing agent[8,9] and also a promising candidate as an energy carrier in fuel cells.[10−13]

Transition-metal ions are known for their ability to facilitate and control O_2 activation, and how dioxygen can be activated by metal complexes remains a central question for chemists.[14,15] In this regard, studies of homogeneous metal-based

Received: May 12, 2015
Published: June 15, 2015

DOI: 10.1021/jacs.5b04917
J. Am. Chem. Soc. 2015, 137, 8644−8653

Scheme 1

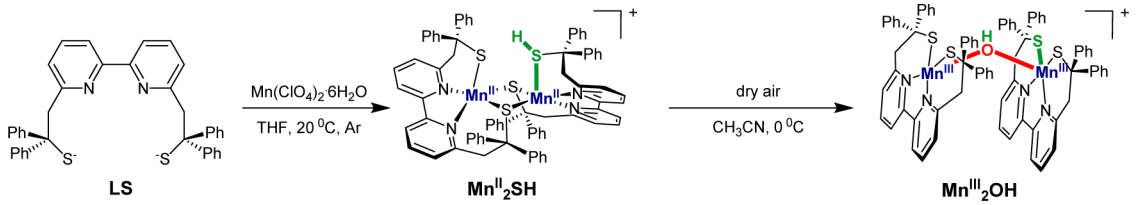

systems are particularly useful for the clarification of mechanistic details of the dioxygen activation process.[16−25] In the specific case of catalytic O_2 reduction, investigations in solution are essential to obtain insights into the factors that control the competition between four- and two-electron reduction processes.[19,26,27]

The reactivity of metal complexes with O_2 is mainly regulated by the nature of the transition metal ion, by the donor atom set supplied by the supporting ligand, and finally by second coordination sphere effects. Among transition metals, manganese exhibits extremely rich oxygen chemistry in both biological and synthetic systems. A number of vital reactions involving dioxygen and its reduced derivatives (superoxide, peroxide, and water) are promoted by Mn-dependent enzymes, including lipoxygenase,[28,29] ribonucleotide reductase,[30] superoxide dismutase,[31] catalases,[32] and the oxygen-evolving complex of Photosystem II.[33] In addition, many synthetic Mn complexes are known to mimic the structure and/or the reactivity of these enzymes.[32,34−36]

The nature of the supporting ligand also plays a key role in the reactivity of metal complexes with dioxygen. In particular, it has been shown that the coordination of thiolates to a metal ion can promote the activation of molecular oxygen[37] for several reasons: (i) stabilization of metal−peroxo,[38−40] −hydroperoxo,[41] −alkylperoxo,[42−44] and −superoxo[45] complexes, as a consequence of thiolate charge donation; (ii) decrease of the activation barrier to O_2 binding, as shown by theoretical studies;[45,46] (iii) assistance of metal oxidation by O_2 by significantly lowering its redox potential;[47] (iv) increase of the basicity of bound substrates by reducing the metal ion Lewis acidity (to generate more basic oxo ligands for instance);[48] and finally (v) stabilization of coordinatively unsaturated M^{II} complexes with the concomitant labilization of the *trans* sites to the thiolate for promoting product release.[47] This has been recently validated by the work of Kovacs et al. in the case of manganese complexes. They reported a series of mononuclear thiolate−Mn^{II} complexes capable of activating and reducing O_2 stoichiometrically by generating mono-μ-oxo dinuclear Mn^{III} species.[38,49] They also detected and characterized the first example of a peroxo-bridged Mn^{III} dinuclear complex as the key intermediate in the process.[38] However, no catalytic studies (oxidation of substrates or dioxygen reduction) were performed on these systems.

In addition to the nature of the metal ion and its first coordination sphere, the control of the secondary coordination sphere of a complex is also crucial to achieve highly functional compounds and high chemical selectivity. In particular, the presence of pendant acids (or bases) is known to promote reactivity via transient hydrogen-bonding interactions, to act as proton relays during a catalytic process, but also to modulate the redox potential of the metal center.[50] In some cases, these concepts have also been validated in the domain of O_2 activation and reduction.[51−54]

In this work, we describe the synthesis and characterization of a rare manganese−thiolate complex, $[Mn^{II}_2(LS)(LSH)]ClO_4$ (**Mn^{II}_2SH**, Scheme 1), bearing a pendant thiol group bound (in its −SH form) to one Mn^{II} ion. This complex is capable of bonding and activating dioxygen. The peculiarity of this complex is that it mediates the reductive cleavage of the O−O bond (four-electron dioxygen reduction) under stoichiometric conditions, while it acts as an active catalyst for two-electron reduction of O_2 in the presence of a proton source and a one-electron reducing agent. The O_2 activation and reduction pathways under both stoichiometric and catalytic conditions have been investigated, leading to insights on the factors that control the competition between four- and two-electron reduction processes.

2. RESULTS

2.1. Synthesis. The potassium salt of the LS ligand (2,2′-(2,2′-bipyridine-6,6′-diyl)bis(1,1-diphenylethanethiolate))[55] reacts with an excess (2.5 equiv) of $Mn(ClO_4)_2·6H_2O$ in THF at 293 K under an inert atmosphere, leading to a pale orange precipitate (see Scheme 1). The resulting powder corresponds to the dimercapto-bridged Mn^{II} dinuclear complex $[Mn^{II}_2(LS)(LSH)]ClO_4$ (**Mn^{II}_2SH**), as shown by single-crystal X-ray diffraction data (*vide infra*). Surprisingly, in this compound, one of the metal-bound thiolates is protonated (i.e., the thiol form). The **Mn^{II}_2SH** complex reacts with O_2 in CH_3CN, leading to the formation of a dark red-purple precipitate, corresponding to the mono-μ-hydroxo dinuclear Mn^{III} complex $[(Mn^{III}_2(LS)_2(OH)]ClO_4$ (**Mn^{III}_2OH**).

2.2. Structural Properties. The X-ray structures of **Mn^{II}_2SH** and **Mn^{III}_2OH** are shown in Figure 1, and selected bond distances and angles are reported in the Supporting Information.

The **Mn^{II}_2SH** cation consists of a dimercapto-bridged dinuclear Mn^{II} complex. Its structure contains a quasi-planar $\{Mn_2S_2\}$ diamond core (deviation from the S2Mn1S52Mn2 plane <0.017 Å, angle between the S2Mn1S52 and S2Mn2S52 planes of 2.36°). The two Mn sites are not equivalent, and each Mn center is pentacoordinated, surrounded by an N2S3 donor set in a distorted square pyramidal geometry. The Mn···Mn distance of 3.1738(6) Å is too long for a direct metal−metal interaction. The discrepancy between the Mn1−S1 and Mn2−S51 bond lengths (2.4399(10) and 2.6462(10) Å, respectively) reflects the fact that S51 is protonated (S51−H51S = 1.61(3) Å), in agreement with the presence of electronic density of a proton found by Fourier transform near S51 (coordinates were refined and isotropic displacement parameter was fixed at 1.2 times that of S51). Coherently, S and Mn K-edge X-ray absorption spectroscopy (XAS) as well as magnetic susceptibility measurements (*vide infra*) demonstrate that both Mn ions are at the +II oxidation state. The S1···S51 distance of 3.772(3) Å is too long for an intramolecular S51−H51S···S1 hydrogen-bond interaction, even if the proton is displaced in an

DOI: 10.1021/jacs.5b04917
J. Am. Chem. Soc. 2015, 137, 8644−8653

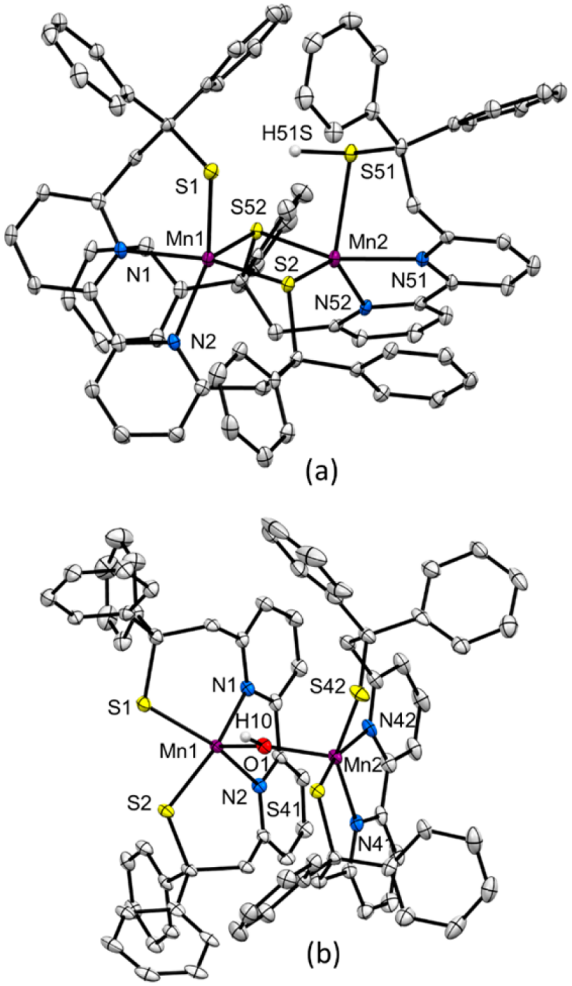

Figure 1. Molecular structures of (a) $\mathbf{Mn^{II}_2SH}\cdot 1.55CH_3CN\cdot 0.45CH_3OH$ and (b) $\mathbf{Mn^{II}_2OH^{\#}}\cdot 7.16CH_3CN$. The thermal ellipsoids are drawn at 30% probability level. All hydrogen atoms, except for H51S in $\mathbf{Mn^{II}_2SH}$ and H10 in $\mathbf{Mn^{III}_2OH^{\#}}$, anions, and solvent molecules are omitted for clarity. Only one crystallographically independent unit of $\mathbf{Mn^{III}_2OH^{\#}}$ is displayed. Selected bond distances (Å) and angles (deg): in $\mathbf{Mn^{II}_2SH}$, Mn1−S1 = 2.4399(10), Mn2−S51 = 2.6462(10); in $\mathbf{Mn^{III}_2OH^{\#}}$, Mn1−O1 = 2.034(3), Mn2−O1 = 2.041(3), Mn1−O1−Mn2 = 146.56(17).

intermediate position between both sulfurs (S1−H51S = 2.22(3) Å, S51−H51···S1 = 159.5(9)°), consistent with a localized proton on one of the monodentate sulfur atoms in the solid state.

The $\mathbf{Mn^{III}_2OH}$ complex crystallizes as a mixed salt, $[(Mn^{III}L)_2(OH)](PF_6)_{0.81}(ClO_4)_{0.19}$ ($\mathbf{Mn^{III}_2OH^{\#}}$), with two crystallographically independent molecules with similar geometries. $\mathbf{Mn^{III}_2OH}$ is a rare example of a dinuclear Mn^{III} complex with a unique hydroxo bridge and the first with thiolate ligands.[56−59] Each manganese(III) ion is surrounded by an N2S2O donor set in a distorted square pyramidal coordination sphere. The Mn^{III}−S distances—with S being unprotonated—are shorter than those in $\mathbf{Mn^{II}_2SH}$, in agreement with the increase of the Mn oxidation state from +II to +III. The Mn−O(H)−Mn angles of 146.56(17)° and 146.11(17)° and the Mn···Mn separations of 3.902(1) Å and 3.903(1) Å are in the range found in the other reported dinuclear μ-OH Mn^{III} complexes (141° < Mn−O−Mn angle < 160° and 3.87 Å < Mn···Mn distance < 3.99 Å).[56−59] A mono-oxo bridge can be excluded on the basis of the Mn···Mn distance that is notably shorter in dinuclear mono-μ-oxo Mn^{III} complexes (3.4−3.6 Å).[34,49,60]

2.3. Mn and S K-Edge XAS Absorption. Mn and S K-edge XAS experiments have been performed to assign the oxidation state of the Mn ions in both $\mathbf{Mn^{II}_2SH}$ and $\mathbf{Mn^{III}_2OH}$ complexes (Figure 2). Such investigation was crucial to indirectly confirm the protonation of one LS ligand in $\mathbf{Mn^{II}_2SH}$ and the hydroxo nature of the bridge present in $\mathbf{Mn^{III}_2OH}$.

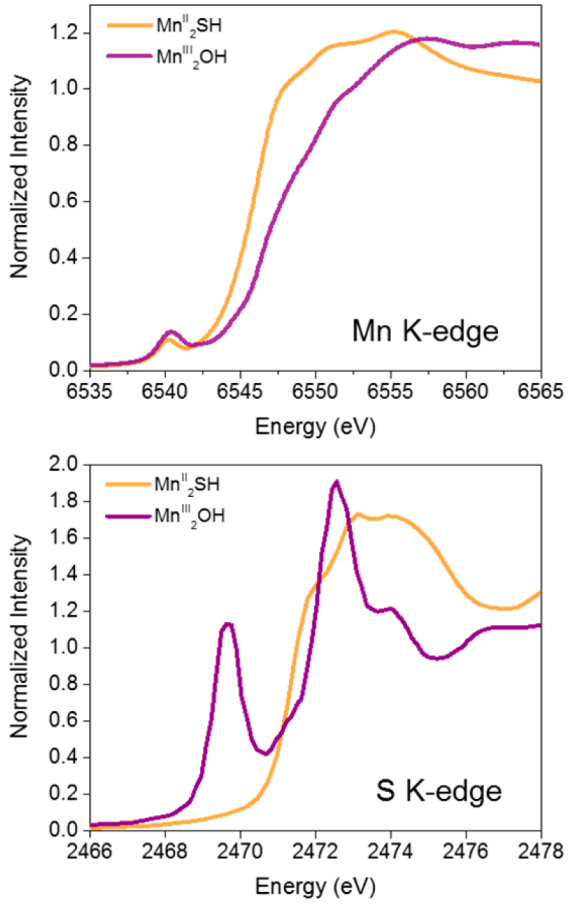

Figure 2. Mn and S K-edge XAS spectra recorded on powdered samples of $\mathbf{Mn^{II}_2SH}$ and $\mathbf{Mn^{III}_2OH}$.

It has been previously shown that the energy of the Mn K-edge (and pre-edge), corresponding to a Mn(1s) → Mn(4p) transition (and Mn(1s) → Mn(3d) transition), is sensitive to the oxidation level of the Mn ions, i.e., the lower the energy, the lower the oxidation state.[61,62] This can be rationalized by considering that removing one electron from an atom that bears a higher positive charge is more difficult. In this specific case, the ∼1.5 eV shift to lower energy of the edge inflection point measured for $\mathbf{Mn^{II}_2SH}$ with respect to that for $\mathbf{Mn^{III}_2OH}$ is consistent with a +II oxidation state in $\mathbf{Mn^{II}_2SH}$ vs +III in $\mathbf{Mn^{III}_2OH}$. The same trend is observed for the much less intense Mn K pre-edge feature at ∼6540 eV.

The sulfur K-edge XAS experiments also provide information on the oxidation level of the Mn ions. In a simplified model, the sulfur K pre-edge corresponds to a transition from the 1s orbital of a sulfur atom to an unoccupied orbital bearing both S 3p and Mn 3d character. It is thus expected that the pre-edge transition shifts to lower energies when the oxidation state of

DOI: 10.1021/jacs.5b04917
J. Am. Chem. Soc. 2015, 137, 8644−8653

the Mn ion increases, as the Mn(3d) orbitals are stabilized in the presence of a higher positive charge on Mn (the S(1s) energy remaining virtually unchanged). Accordingly, a sulfur K pre-edge is observed only in the case of $\mathbf{Mn^{III}_2OH}$, at an energy of 2469.6 eV, while that of $\mathbf{Mn^{II}_2SH}$ is obscured by the edges above 2472 eV. For both complexes, the sulfur K-edge energies at approximately 2472 eV are consistent with reduced sulfurs as thiol or thiolate groups.

2.4. Magnetic Properties. Variable-temperature magnetic susceptibility data were collected on powdered samples of $\mathbf{Mn^{II}_2SH}$ and $\mathbf{Mn^{III}_2OH}$ in the 1.8 to 300 K temperature range at 1000 Oe (Figure 3).

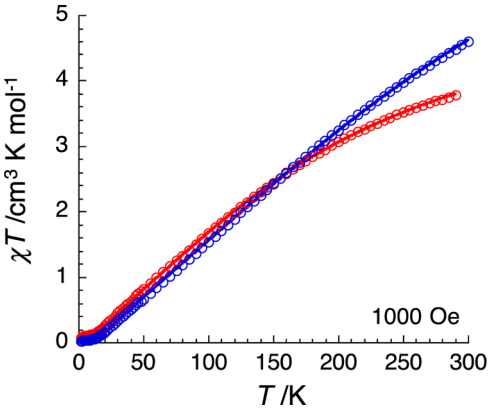

Figure 3. Temperature dependence of the χT product (where χ is the molar magnetic susceptibility equal to M/H per complex) measured at 1000 Oe for $\mathbf{Mn^{II}_2SH}\cdot 1.55CH_3CN\cdot 0.45CH_3OH$ (blue circles) and $\mathbf{Mn^{III}_2OH^{\#}}\cdot 7.16CH_3CN$ (red circles). The solid lines are the best fits of the experimental data to the models described in the text.

For both systems, the steady decrease of χT product to nearly zero at 2 K suggests the presence of significant intra-complex antiferromagnetic exchange. Therefore, the magnetic data were analyzed by an isotropic spin-dimer Heisenberg model, $H = -2JS_AS_B$, assuming that the two metal ions are high spin Mn^{II} ($S_A = S_B = 5/2$) in $\mathbf{Mn^{II}_2SH}$, or high spin Mn^{III} ($S_A = S_B = 2$) in $\mathbf{Mn^{III}_2OH}$.[63] Concerning $\mathbf{Mn^{II}_2SH}$, the bridging thiolate ligands mediate antiferromagnetic interactions between Mn^{II} magnetic centers leading to a diamagnetic $S = 0$ ground state. The resulting best fit for $\mathbf{Mn^{II}_2SH}$ (solid blue line in Figure 3) gives $g_A = g_B = 2.05(8)$ and $J = -22(1)$ cm^{-1} ($-31(1)$ K). The magnetic coupling between two Mn^{II} ions is typically small ($J < 10$ cm^{-1}) regardless of the nature of the bridging ligand[32,64] (We note that phenolato bridges are an exception).[65] Therefore, the exchange interaction found in $\mathbf{Mn^{II}_2SH}$ is surprisingly high. In the literature, the number of polynuclear Mn^{II} complexes with thiolate bridge(s) is limited and, to the best of our knowledge, the magnetic properties have been reported only for one of those, i.e., a linear trinuclear Mn^{II} complex with a mono-μ-thiolato bridge between each Mn ion, with a relatively strong antiferromagnetic interaction evaluated around -9.8 cm^{-1}.[66] Concerning $\mathbf{Mn^{III}_2OH}$, the resulting best fit affords $g_A = g_B = 2.00(5)$ and $J = -19(1)$ cm^{-1} ($-27(1)$ K; solid red line in Figure 3). The magnetic properties of only two other mono-μ-hydroxo dinuclear Mn^{III} complexes have been reported so far, both containing porphyrin-based ligands. In these two complexes, the antiferromagnetic exchange interaction is much larger, i.e., -71 cm^{-1} and -74 cm^{-1}, consistent with larger Mn−O−Mn angle values (152.73° and 160.4°, respectively, vs 146.56° and 146.11° for $\mathbf{Mn^{III}_2OH}$).[56,57]

2.5. Solution Properties of $\mathbf{Mn^{II}_2SH}$. The dinuclear solid-state structure of $\mathbf{Mn^{II}_2SH}$ is retained when dissolved in CH_3CN, as attested by electrospray ionization mass spectrometry (ESI-MS; 1267.2 m/z). The redox properties of $\mathbf{Mn^{II}_2SH}$ have been investigated by cyclic voltammetry (CV) in CH_3CN (Figure 4 and Supporting Information).

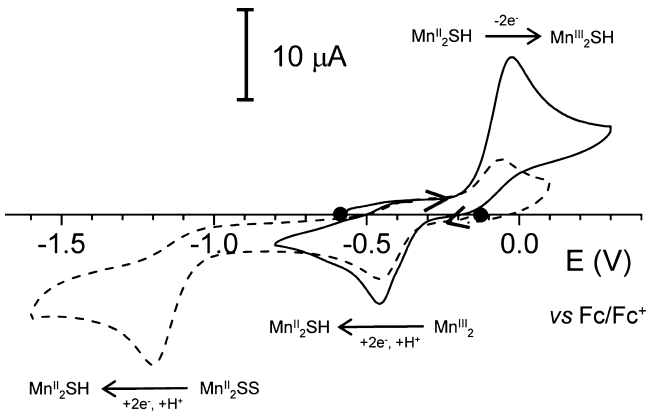

Figure 4. CV of $\mathbf{Mn^{II}_2SH}$ (0.7 mM) in CH_3CN, 0.1 M Bu_4NPF_6, before (—) and after (---) electrolysis at +0.05 V.

First, the presence of the metal-bound SH group (*vide supra*) has been evidenced in solution. A cathodic peak at −1.27 V vs Fc/Fc^+ is observed only in the CV of $\mathbf{Mn^{II}_2SH}$ recorded on Pt working electrode, but not on glassy carbon, GC. The well-known ability of platinum to lower the overpotential for proton reduction leads to the assignment of this peak to the reduction of the Mn-bound thiol proton. Second, the CVs of $\mathbf{Mn^{II}_2SH}$ recorded both on Pt or GC electrodes show an irreversible anodic peak at $E_{pa} = -0.01$ V, assigned to a two-electron metal-based oxidation, $Mn^{II}Mn^{II} \rightarrow Mn^{III}Mn^{III}$. The redox potential associated with the $Mn^{II}Mn^{II}/Mn^{III}Mn^{III}$ system suggests that $\mathbf{Mn^{II}_2SH}$ could be easily oxidized by O_2, in analogy to the mononuclear Mn^{II}-thiolate complexes reported by Kovacs (for which $E_{1/2} = +0.08$ to $+0.20$ V vs Fc/Fc^+ for the Mn^{III}/Mn^{II} redox couples). The potential of the corresponding cathodic peak ($E_{pc} = -0.47$ V) indicates that the electrochemically generated $Mn^{III}Mn^{III}$ dinuclear complex ($\mathbf{Mn^{III}_2SH}$) undergoes a fast chemical rearrangement, probably associated with the deprotonation of the thiol group. A different redox behavior was observed in the case of a related dinuclear Cu^I complex containing an analogous bis-μ-thiolato bridge. The latter displayed a one-electron reversible $Cu^{1.5}Cu^{1.5}/Cu^ICu^I$ redox process, the mixed-valence species being stable and fully characterized.[67] In the case of $\mathbf{Mn^{II}_2SH}$, the generation of the mixed-valence species is prevented presumably due to the fact that the redox potential of the $Mn^{III}Mn^{II}/Mn^{II}Mn^{II}$ couple is too close to that of the corresponding $Mn^{III}Mn^{III}/Mn^{III}Mn^{II}$ one.

During the oxidative electrolysis of $\mathbf{Mn^{II}_2SH}$ in CH_3CN (at $E = +0.05$ V), the color of the solution turns from light orange to deep orange and then evolves to light yellow at 293 K. This final species corresponds to a Mn^{II}_2-disulfide complex that has been isolated and characterized and will be described in a separate contribution (see Supporting Information). On this basis, the deep orange intermediate species (that can be stabilized at 253 K) has been assigned to a bis-μ-thiolato

DOI: 10.1021/jacs.5b04917
J. Am. Chem. Soc. 2015, 137, 8644−8653

dinuclear Mn^{III} complex with two terminal thiolate groups ($\mathbf{Mn^{III}_2}$), the isoelectronic form of the Mn^{II}_2-disulfide complex. The deep orange color is due to a broad absorption band at ~475 nm (~6400 M^{-1} cm^{-1}, Figure 5) and was assigned to

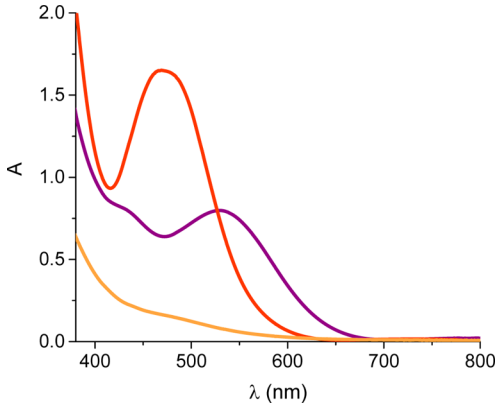

Figure 5. UV−vis spectrum of $\mathbf{Mn^{II}_2SH}$ (0.35 mM) in CH_3CN before (orange trace) and after (purple trace) addition of 1 mM O_2 to generate $\mathbf{Mn^{III}_2OH}$. $\mathbf{Mn^{III}_2}$ is obtained after the addition of 2,6-lutidinium tetrafluoroborate (1 equiv) to $\mathbf{Mn^{III}_2OH}$, (red trace); 1 cm optical path length.

ligand-to-metal charge transfer (LMCT) contributions to the lower-energy d-d transitions based on time-dependent density functional theory (TDDFT) calculations (see Supporting Information).

2.6. Reactivity of Mn^{II}_2SH with Dioxygen and Catalytic Production of H_2O_2. When a light orange solution of $\mathbf{Mn^{II}_2SH}$ (1 mM) is exposed to air (see video in the Supporting Information) or to dry O_2 (~1 mM) in CH_3CN at 293 K, a dark red-purple solution is formed, containing the structurally characterized $\mathbf{Mn^{III}_2OH}$ complex as the main product (Scheme 1, Figure 1). Based on the ε value of $\mathbf{Mn^{III}_2OH}$ at 527 nm (~3100 M^{-1} cm^{-1}) determined from the isolated product, about ~70% of $\mathbf{Mn^{III}_2OH}$ is generated under these conditions. The low stability of the product at 293 K can explain the non-quantitative character of the process as well as the possible presence of weak absorbers as side-products. Based on TDDFT calculations, the 527 nm absorption band has been assigned to a mixed d−d/intraligand charge transfer (ILCT) transition (Supporting Information). In agreement with its dinuclear structure, the CV of $\mathbf{Mn^{III}_2OH}$ displays two successive one-electron reduction processes at E_p = −0.60 V (ΔE_p = 80 mV) and −0.75 V (ΔE_p = 80 mV) corresponding to the stepwise reduction of the Mn^{III} dinuclear complex into the corresponding Mn^{II} analogue (see Supporting Information).

In an attempt to identify O_2 as the source of oxygen for the hydroxo bridge, $^{18}O_2$ was used to generate $\mathbf{Mn^{III}_2OH}$. Even though no labeled $\mathbf{Mn^{III}_2{}^{18}OH}$ compound was observed by ESI-MS, H_2O has been excluded as the oxygen source in $\mathbf{Mn^{III}_2OH}$ based on the fact that no $\mathbf{Mn^{III}_2OH}$ is formed when $\mathbf{Mn^{III}_2}$ is electrochemically generated in the presence of H_2O. The lack of ^{18}O-labeling in $\mathbf{Mn^{III}_2OH}$ when $^{18}O_2$ is used has been attributed to a fast exchange between the μ-^{18}OH bridge and adventitious water as previously reported for the $Mn^{III/IV}_4$-oxo complex of the Photosystem II.[68,69] Such exchange has been further evidenced by adding $H_2{}^{18}O$ to $\mathbf{Mn^{III}_2OH}$ in CH_3CN (see Supporting Information).

In order to evaluate the potential catalytic activity of $\mathbf{Mn^{II}_2SH}$ for proton-assisted O_2 reduction, the effect of proton addition during the oxygenation process has been monitored by visible absorption spectroscopy (Figure 5) and CV. In a first step, $\mathbf{Mn^{III}_2OH}$ is generated from the reaction of $\mathbf{Mn^{II}_2SH}$ with O_2. The following addition of 2,6-lutidinium tetrafluoroborate ($LutHBF_4$) instantaneously leads to the protonation of $\mathbf{Mn^{III}_2OH}$ with the simultaneous production of H_2O and $\mathbf{Mn^{III}_2}$ (Scheme 2a). Subsequently, the *in situ* generated $\mathbf{Mn^{III}_2}$

Scheme 2

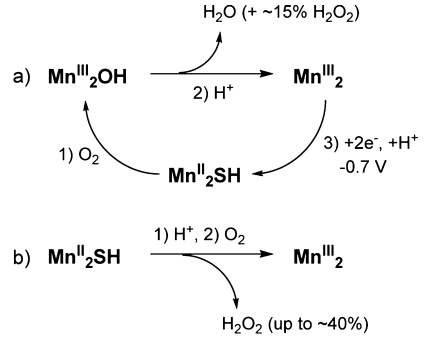

complex can be reduced by exhaustive electrolysis at E = −0.7 V vs Fc/Fc^+, to partially recover the initial $\mathbf{Mn^{II}_2SH}$ complex, thus completing one stepwise cycle. The incomplete recovery of $\mathbf{Mn^{II}_2SH}$ (only ~35%, as estimated by the initial and final CVs) can be mainly ascribed to the poor stability of $\mathbf{Mn^{III}_2}$ at 293 K (this species evolves to a Mn^{II}_2-disulfide complex, *vide supra*).

Coherently, when $\mathbf{Mn^{II}_2SH}$ reacts with O_2 in the presence of $LutHBF_4$ (up to 50 equiv), the direct formation of $\mathbf{Mn^{III}_2}$ is observed. Under such conditions, the concomitant production of H_2O_2, up to ~40% vs $\mathbf{Mn^{II}_2SH}$, is attested by titration with the H_2O_2-specific Ti-TPyP reagent[70,71] (see Supporting Information) or with iodide under acidic medium. The amount of H_2O_2 formed depends on the relative concentration of acid versus $\mathbf{Mn^{II}_2SH}$: the higher the $LutHBF_4$:$\mathbf{Mn^{II}_2SH}$ ratio, the larger the amount with a plateau for 20:1 ratio (see Discussion). Production of 15% H_2O_2 is detected in the absence of acid: this has been attributed to the fact that the Mn-bound pendant thiol can act as a proton source for a neighboring complex molecule.

As a further step, we have investigated the catalytic activity of the $\mathbf{Mn^{III}_2}$/$\mathbf{Mn^{II}_2SH}$ system for O_2 reduction using a sacrificial electron donor and protons.[16,19,72,73] As one-electron reducing agents, we have selected octamethylferrocene (Me_8Fc) and decamethylferrocene ($Me_{10}Fc$), for their standard potential ($E_{1/2}$ Me_8Fc^+/Me_8Fc = −0.40 V, $E_{1/2}$ $Me_{10}Fc^+/Me_{10}Fc$ = −0.49 V) that should be suitable to reduce $\mathbf{Mn^{III}_2}$ (E_{pc} = −0.47 V). The addition of a catalytic amount of $\mathbf{Mn^{II}_2SH}$ (100 μM) to an air-saturated CH_3CN solution of Me_nFc (n = 8 or 10, 2 mM, 20 equiv) and $LutHBF_4$ (15 mM, 150 equiv) at 293 K results in the quantitative and efficient oxidation of the ferrocene derivatives by O_2 to afford octamethylferricenium (Me_8Fc^+) and decamethylferricenium ($Me_{10}Fc^+$), respectively. Figure 6 shows the absorption spectral changes during the catalytic reaction and the corresponding time profiles for the generation of Me_8Fc^+ and $Me_{10}Fc^+$ (at 750 and 778 nm, respectively). In the absence of the catalyst, oxidation of the ferrocene derivatives occurs only to an insignificant extent. Under such conditions, the rate of electron transfer to $\mathbf{Mn^{III}_2}$ follows pseudo-zero-order kinetics in the case of Me_8Fc, while it becomes pseudo-first-order kinetics with $Me_{10}Fc$. This can be

DOI: 10.1021/jacs.5b04917
J. Am. Chem. Soc. 2015, 137, 8644−8653

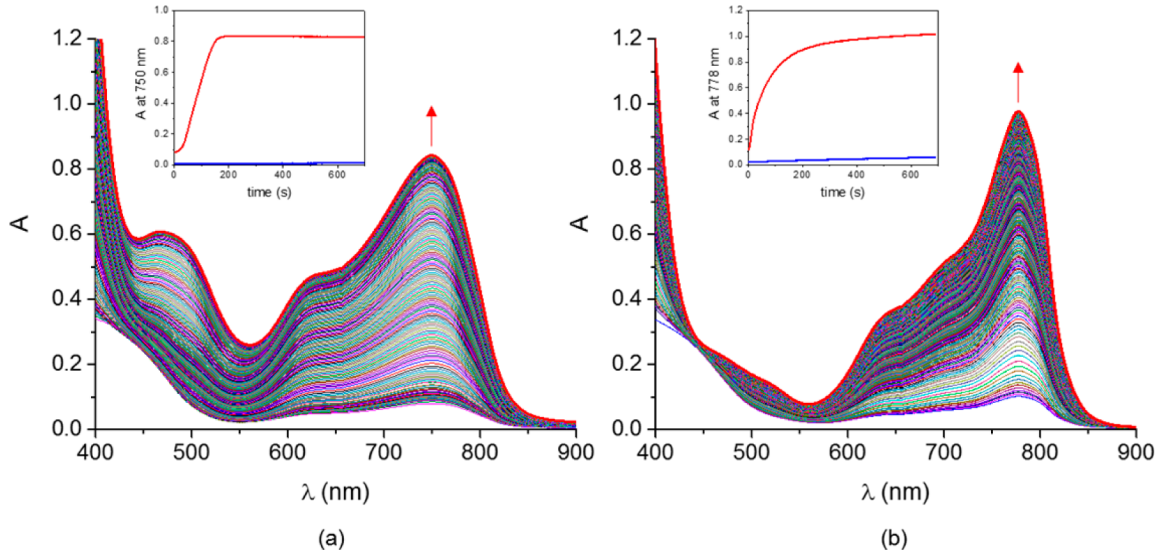

Figure 6. UV−vis spectral changes observed during the two-electron O_2 reduction catalyzed by $\mathbf{Mn^{II}_2SH}$ with Me_nFc ((a) n = 8, (b) n = 10) in the presence of $LutHBF_4$ in CH_3CN at 293 K (air-saturated solution, 2.0 mM Me_nFc, 15 mM $LutHBF_4$, 100 μM $\mathbf{Mn^{II}_2SH}$, 1 cm path length). The insets show the time profiles for Me_8Fc^+ and $Me_{10}Fc^+$ formation (red trace, absorbance at 750 and 778 nm, respectively); the profiles of the corresponding blank samples (no catalyst) are also shown (blue trace).

Scheme 3. Proposed Pathways for Proton-Coupled Two-Electron O_2 Reduction Catalyzed by Mn^{II}_2SH in the Presence of Me_nFc (n = 8 or 10) (Left) and for Four-Electron O_2 reduction by Mn^{II}_2SH in Stoichiometric Conditions (Right)[a]

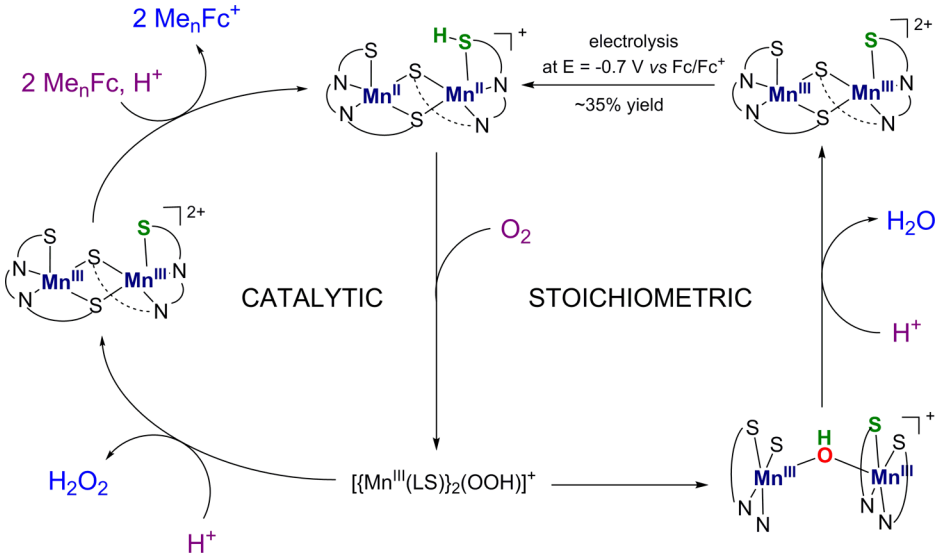

[a]Reagents and products are indicated in purple and in blue, respectively.

tentatively explained by a difference of steric hindrance between both reducing agents by limiting the interaction between the two complexes, $\mathbf{Mn^{III}_2}$ being very bulky with the presence of eight phenyl groups in the ligands.

In addition, the nature of the oxygen-reduction product and the selectivity of the catalytic process was investigated. After the completion of catalysis, a 0.6 mM concentration of H_2O_2 was detected in the sample solution when the substrate was Me_8Fc (titration with the Ti-TPyP reagent; see Supporting Information).[70,71] In contrast, no H_2O_2 formation was observed in the case of $Me_{10}Fc$. It has, however, been shown that H_2O_2 can spontaneously decompose, partially or completely, in the presence of ferrocene derivatives.[19] We have estimated that in the present conditions about 30% of H_2O_2 formed during the catalytic oxidation of Me_8Fc is decomposed. By taking into account this correction, a ~43% yield of H_2O_2 vs Me_8Fc is produced by O_2 reduction at 293 K. In the case of $Me_{10}Fc$, low-temperature experiments have been carried out, in propionitrile and acetone at 223 K (see Supporting Information) in order to prevent the direct oxidation of $Me_{10}Fc$ by H_2O_2. Under these conditions, a ~40% of H_2O_2 vs $Me_{10}Fc$ is produced in both solvents. Taking into account the stoichiometry of the two-electron reduction of O_2 by ferrocene derivatives (eq 1), the amount of H_2O_2 detected corresponds to ~80−84% selectivity. (We note that 50% H_2O_2 vs Me_nFc is expected for a completely selective process.)

$$O_2 + 2Me_nFc + 2H^+ \rightarrow 2Me_nFc^+ + H_2O_2 \quad (1)$$

In summary, in the presence of $\mathbf{Mn^{II}_2SH}$ as catalyst, both Me_8Fc and $Me_{10}Fc$ are quantitatively oxidized by O_2 to give the

DOI: 10.1021/jacs.5b04917
J. Am. Chem. Soc. 2015, 137, 8644−8653

corresponding Me_nFc^+ cation, with O_2 selectively reduced to hydrogen peroxide.

3. DISCUSSION

3.1. Mn^{II}_2SH: An Unusual Metal−Thiol System. In coordination chemistry, although metal-bound thiolates (M−S) are very common, examples of metal-bound thiols (M−SH) are relatively rare. Among the structurally characterized M−SH complexes, most examples are based on iron[32,33] or ruthenium.[34,35] The formation of transient metal−thiol bonds in the active sites of metalloenzymes, including [NiFe][36] and [FeFe][37] hydrogenases, nitrogenase,[38] and their biomimetic models, is often proposed (and in some cases established) to be an influential factor in their reactivity. In these systems, metal-bound thiols can act as proton relay during the catalytic process, but are also capable of tuning the redox potential of the active metal centers. Concerning the O_2 activation domain, one Mn^I complex containing a pendant thiol is reported to react with O_2, leading to the formation of a mononuclear O_2 side-on-bound Mn^{IV} complex.[39] However, in this case the pendant proton does not seem to take part in the reactivity of the system.

In **Mn^{II}_2SH**, the presence of one coordinated thiol has been unambiguously demonstrated both in the solid state (as evidenced by the Mn2−S51 distance in the X-ray structure and, indirectly, by magnetic and XAS measurements) and in solution (as shown by CV), with the hexaaqua Mn(II) as the most probable proton source. The uncommon stability of the terminal metal-bound thiol in solution could be attributed to an intramolecular SH···S bond interaction between S1 and S51 (see Figure 1). The presence of a stabilizing intramolecular interaction is supported by DFT calculations (see Supporting Information). Interestingly, the protonation induces a remarkable increase of the oxidation potential of the Mn^{II} dinuclear complex (of ∼300 mV, data not shown), resulting from the lower donor ability of a thiol functionality with respect to a thiolate. In the case of a reported Ni^{II}−thiol(ate) complex,[39] a similarly large proton-induced shift in the redox potentials (+250 mV) has been previously observed without notable structural modifications.

3.2. Proposed O_2 Reduction Pathway(s) with Mn^{II}_2SH under Stoichiometric and Catalytic Conditions. Under stoichiometric conditions and in the absence of an external proton source (Scheme 3, right), the reaction between **Mn^{II}_2SH** and dioxygen generates the μ-hydroxo complex **Mn^{III}_2OH**. In this case, the O−O bond reductive cleavage and full four-electron reduction of O_2 are achieved. Dioxygen activation is probably promoted by the fact that a coordination vacancy can be created on each Mn center of **Mn^{II}_2SH** by breaking the two μ-S bridges. It can then be proposed that the formation of **Mn^{III}_2OH** follows an oxygenation process parallel to those described for Fe^{II} porphyrins.[74] In those systems, a Fe^{III}_2−peroxo intermediate evolves into a μ-oxo Fe^{III} dimer as a consequence of O−O bond cleavage via a bimolecular process. In this respect, Kovacs has recently isolated and crystallized the first example of peroxo-bridged Mn^{III} dinuclear complex.[38] Efforts to detect and characterize a similar intermediate are ongoing and computations are being pursued in order to assess its energetic accessibility.

When protons ($LutHBF_4$) are added on a freshly prepared **Mn^{III}_2OH** solution, its μ-hydroxo bridge is immediately protonated to afford **Mn^{III}_2** and H_2O. In the case of the dinuclear μ-oxo thiolate Mn^{III} complexes described by Kovacs et al., concomitant addition of ROH is required to release water.[75] In our system, the release of water is driven by the tendency of the complex to form μ-S bridges.

When a proton source ($LutHBF_4$) is already present in the initial solution of **Mn^{II}_2SH**, an alternative reaction pathway can be followed. Under these conditions the postulated Mn^{III}_2−(hydro)peroxo intermediate ($[\{Mn^{III}(LS)\}_2(OOH)]^+$ in Scheme 3) reacts with protons favoring the cleavage of the Mn−O bond and the subsequent formation of hydrogen peroxide (up to 40% vs **Mn^{II}_2SH** (Scheme 3, left). This two-electron O_2 reduction pathway coexists with the reductive cleavage of the O−O bond leading to the same final **Mn^{III}_2** product. Two key factors regulate the competition between O−O and M−O rupture in metal−peroxo complexes: (i) the intrinsic strength of the O−O and M−O bonds and (ii) the presence of a proton source. Regarding the first aspect, the O−O bond lengths of previously reported thiolate Mn^{III}−peroxo and Mn^{III}−alkylperoxo complexes (1.431(5)−1.468(7) Å)[38,42,43] fall in the high limit of those observed for metal−peroxo complexes. These long bond distances are consistent with highly activated O−O bonds that are easy to cleave. On the other hand, regulation of proton delivery to a metal−peroxo species is also crucial in the competition between M−O vs O−O ruptures. As shown in the case of classical copper systems,[76,77] and also for a side-on peroxo−Mn^{III} mononuclear complex,[78] more acidic media favor M−O rupture, while in less acidic media, the O−O bond is cleaved. Our experimental data are in full agreement with previous findings: while the presence of thiolate ligands favors the O−O breaking, the addition of protons ($LutHBF_4$) promotes the M−O rupture.

The catalytic O_2 reduction process presented herein, in which Me_nFc are used as monoelectronic sacrificial donors and **Mn^{II}_2SH** as catalyst, represents a rare example of manganese-based molecular catalyst for two-electron reduction of O_2 in homogeneous solution.[79−81]

The proposed mechanism of H_2O_2 formation, depicted in Scheme 3, left, is most likely the same as that of the stoichiometric reaction in acidic medium. When compared to the stoichiometric process, the higher selectively for H_2O_2 is consistent with the presence of a larger excess of acid (200 equiv vs the Mn catalyst) and higher dilution conditions (100 μM of **Mn^{II}_2SH**) that disfavor the bimolecular process proposed to generate **Mn^{III}_2OH**. Regeneration of the initial complex (Scheme 3, left) occurs by electron transfer from Me_nFc (n = 8 or 10) to **Mn^{III}_2**. This process should be thermodynamically feasible in both cases ($\Delta G \approx +0.05$ eV and −0.04 eV for Me_8Fc $Me_{10}Fc$, respectively).[16] The process is further driven by protonation of the reduced product to afford **Mn^{II}_2SH**. Even though **Mn^{III}_2** is relatively unstable (as it slowly decays to a Mn^{II}_2−disulfide complex), under catalytic conditions the presence of an excess of Me_nFc (20 equiv) permits its immediate reduction, thus circumventing its decomposition. It is worth noting that **Mn^{III}_2** is not accumulated during the catalytic process, as the corresponding absorption band at ∼475 nm is not observed during the catalysis (Figure 6).

4. CONCLUSION

Herein, we describe a new thiolate-bridged dimanganese(II) complex, $[Mn^{II}_2(LS)(LSH)]ClO_4$ (**Mn^{II}_2SH**), which represents an unusual system with a metal-bound pendant thiol (M−SH). This complex is capable of binding and activating dioxygen. In particular, under stoichiometric conditions and in the absence

DOI: 10.1021/jacs.5b04917
J. Am. Chem. Soc. 2015, 137, 8644−8653

of an external proton source, $\mathbf{Mn^{II}_2SH}$ reacts with dioxygen to generate a μ-hydroxo complex, $[(Mn^{III}_2(LS)_2(OH)]ClO_4$ ($\mathbf{Mn^{III}_2OH}$). In this case the reductive cleavage of the O−O bond is achieved, leading to a four-electron O_2 reduction process. Conversely, in the presence of a proton source and of a one-electron reducing agent, $\mathbf{Mn^{II}_2SH}$ selectively catalyzes the reduction of dioxygen to hydrogen peroxide. The rupture of the M−O bond in the putative manganese−peroxo intermediate is favored by the acidic medium, leading to two-electron O_2 reduction. The $\mathbf{Mn^{II}_2SH}$ complex represents a rare example of manganese-based molecular catalysts for selective two-electron O_2 reduction in homogeneous solution.[79−81] Current efforts in our group are directed to investigate the role and influence of the Mn-bound pendant thiol on the oxygen chemistry of $\mathbf{Mn^{II}_2SH}$.

5. EXPERIMENTAL SECTION

H_2L was prepared according to a reported procedure.[55] All other reagents and solvents were used as received. THF was distilled over Na/benzophenone prior to use. Acetonitrile (99.9+ %, extra dry) was distilled over CaH_2 prior to use. The synthesis of the complexes was performed under argon (in a glovebox with <5 ppm of O_2 for $\mathbf{Mn^{II}_2SH}$, and in a Schlenk tube for $\mathbf{Mn^{III}_2OH}$). ***Caution!*** *Perchlorate salts of metal complexes are potentially explosive. Only small quantities of material should be prepared, and the samples should be handled with care.* The elemental analyses were carried out with a C, H, N analyzer (SCA, CNRS). The ESI-MS spectra were registered on a Bruker Esquire 3000 Plus ion trap spectrometer equipped with an ESI source. The samples were analyzed in positive ionization mode by direct perfusion in the ESI-MS interface (ESI capillary voltage = 2 kV, sampling cone voltage = 40 V). The electronic absorption spectra were recorded on a Varian Cary 300 absorption spectrophotometer in quartz cells (optical path length = 1 cm).

5.1. Synthesis of $[Mn^{II}_2(LS)(LSH)]ClO_4$ ($\mathbf{Mn^{II}_2SH}$). Solid KH (30% in mineral oil, 150 mg, 1.122 mmol) was added to a solution of H_2L (200 mg, 0.344 mmol) in THF (10 mL). After 20 min, the excess of KH was filtered off, and a solution of $Mn(ClO_4)_2{\cdot}6H_2O$ (310 mg, 0.856 mmol) in THF (5 mL) was slowly added to the yellow solution under stirring. During the addition, the color of the solution turned to dark brown, and subsequently to orange. After a few minutes, a pale orange precipitate was formed. After 1 h, this solid was separated from the mother liquid by filtration and extracted with dichloromethane (3 × 5 mL). The solvent was removed in vacuo, and the residual solid was washed with THF (3 mL), dried, and collected as an pale orange powder ($\mathbf{Mn^{II}_2SH}$, 182 mg, 0.133 mmol, 77%). ESI-MS (5×10^{-4} M, CH_3CN, *m/z*, I%): 633.2, 100 $[MnL]^+ + [Mn_2L(LH)]^{2+}$; 1267.2, 95 $[Mn_2L_2]^+$. Anal. Calcd for $C_{76}H_{61}N_4S_4Mn_2ClO_4{\cdot}0.5KClO_4$ (1437.19): C, 63.51; H, 4.28; N, 3.90. Found: C, 63.40; H, 4.36; N, 3.79. Absorption spectrum in CH_3CN (λ_{max}, nm (ε, M^{-1} cm^{-1})): 309 (~250 00). X-ray-suitable orange-brown single crystals corresponding to $\mathbf{Mn^{II}_2SH}{\cdot}1.55CH_3CN{\cdot}0.45CH_3OH$ were obtained by slow diffusion of diethyl ether into a solution of the product in acetonitrile at 293 K.

5.2. Synthesis of $[Mn^{III}_2(LS)_2(OH)]ClO_4$ ($\mathbf{Mn^{III}_2OH}$). A suspension of $\mathbf{Mn^{II}_2SH}$ (30 mg, 0.021 mmol) in acetonitrile (10 mL) in the presence of 0.2 M Bu_4NClO_4 was cooled to 0 °C. Dry air (10 mL, 293 K, 0.086 mmol O_2) was added, yielding a dark red-violet solution. *Note that, when vigorous bubbling of O_2 is carried out on a $\mathbf{Mn^{II}_2SH}$ solution, $\mathbf{Mn^{III}_2OH}$ is not the main product of the reaction.* After a few minutes, a dark red-purple precipitate was formed. After stirring for 1 h at 0 °C, this solid was filtered, washed with acetonitrile (2 × 2 mL), dried, and collected as a dark red-purple powder ($\mathbf{Mn^{III}_2OH}$, 18 mg, 0.013 mmol, 62%). ESI-MS (6.5×10^{-5} M, CH_3CN, *m/z*, I%): 633.3, 16 $[MnL]^+ + [Mn_2L(LH)]^{2+}$; 1283.5, 100 $[(MnL)_2OH]^+$. Anal. Calcd for $C_{76}H_{61}N_4S_4Mn_2OClO_4$ (1383.92): C, 65.95; H, 4.44; N, 4.05. Found: C, 66.06; H, 4.57; N, 3.91. Absorption spectrum in CH_3CN (λ_{max}, nm (ε, M^{-1} cm^{-1})): 311 (~27 500), 530 (~4300). $\mathbf{Mn^{III}_2OH}$ crystallizes from the following procedure: 1.5 equiv of dioxygen were added into a 0.9 mM solution of $\mathbf{Mn^{II}_2SH}$ in acetonitrile at −18 °C, in the presence of 0.02 M Bu_4PF_6, without stirring. After a few days, X-ray-suitable dark red single crystals of the product were obtained, corresponding to $[(Mn^{III}L)_2(OH)](PF_6)_{0.81}(ClO_4)_{0.19}$ ($\mathbf{Mn^{III}_2OH^{\#}}$)·$7.16CH_3CN$.

5.3. Catalytic Experiments. The oxidation of Me_nFc (n = 8,10) by O_2 in the presence of a catalytic amount of $\mathbf{Mn^{II}_2SH}$ and an excess of 2,6-lutidinium tetrafluoroborate ($LutHBF_4$) was monitored by visible absorption spectroscopy in CH_3CN at 293 K for both Me_8Fc and $Me_{10}Fc$, and in propionitrile and acetone at 233 K for $Me_{10}Fc$. In a typical experiment (see Figure 6), an air-saturated solution of $LutHBF_4$ (25 μL, 2.0 M) was added to an air-saturated solution of Me_nFc (2.225 mL, 2.24 mM), in the presence of air (1 atm, 0.21 atm O_2), in a septum-sealed 1 cm quartz cuvette kept at 293 K or at 233 K by a cryostat. After the sample was stirred stirring for 5 s, an Ar-saturated solution of $\mathbf{Mn^{II}_2SH}$ (250 μL, 1.0 mM) was added under stirring (air-saturated, 2.0 mM Fc*, 15.0 mM $LutHBF_4$, 100 μM $\mathbf{Mn^{II}_2SH}$). The increase in the absorbance of a band at 750 or 778 nm (corresponding to the formation of the Me_nFc^+ ion for Me_8Fc and $Me_{10}Fc$, respectively) was monitored with time by using an MCS 501 UV-NIR (Carl Zeiss) photodiode-array spectrophotometer (Δt = 1 s). The corresponding blank experiment was performed in the same conditions, by adding degassed solvent (250 μL) instead of the $\mathbf{Mn^{II}_2SH}$ solution. The ε values for the absorption maxima of Me_nFc^+, required to determine the concentration of formed Me_nFc^+ in the samples, were estimated by the electron-transfer oxidation of Me_nFc with $AgBF_4$ ($\varepsilon_{750}(Me_8Fc^+)$ = 383 M^{-1} cm^{-1}, $\varepsilon_{778}(Me_{10}Fc^+)$ = 495 M^{-1} cm^{-1}). All the experiment were repeated three times, obtaining highly reproducible data (in the 5% range).

5.4. Detection of H_2O_2 by the Ti-TPyP reagent. *5.4.1. Stoichiometric Conditions.* A series of sample solutions, containing $\mathbf{Mn^{II}_2SH}$ (0.8 mM) in CH_3CN, in the presence of different equivalents (0, 5, 10, 20, 30, 40, 50) of $LutHBF_4$, were prepared under argon (glovebox) and stirred under air for 3 min before analysis.

5.4.2. Catalytic Conditions. Samples were prepared as described in the previous paragraph (air-saturated solution, 2.0 mM Me_nFc, 15.0 mM $LutHBF_4$, 100 μM $\mathbf{Mn^{II}_2SH}$) at 293 K in CH_3CN (Me_8Fc and $Me_{10}Fc$) and at 233 K in propionitrile or acetone ($Me_{10}Fc$) and analyzed after reaction completion.

5.4.3. Method. The amount of produced hydrogen peroxide in the samples was determined by spectroscopic titration with an acidic solution of $[TiO(tpypH_4)]^{4+}$ complex (Ti-TPyP reagent).[70] The detailed procedure is reported in the Supporting Information.

■ ASSOCIATED CONTENT

Ⓢ Supporting Information

Additional experimental and computational details; data related to the experimental and calculated structural properties of the complexes, to their electrochemical properties, and to the reactivity of the complex in stoichiometric and catalytic conditions; analysis of the absorbance properties of $\mathbf{Mn^{III}_2OH}$ and $\mathbf{Mn^{III}_2}$ by TDDFT; and CIF files for $\mathbf{Mn^{II}_2SH}$ and $\mathbf{Mn^{III}_2OH}$. The Supporting Information is available free of charge on the ACS Publications website at DOI: 10.1021/jacs.5b04917.

■ AUTHOR INFORMATION

Corresponding Authors

*marcello.gennari@ujf-grenoble.fr

*carole.duboc@ujf-grenoble.fr

Present Address

□C.J.P.: Department of Chemistry, The Pennsylvania State University, University Park, PA 16802, United States

Notes

The authors declare no competing financial interest.

DOI: 10.1021/jacs.5b04917
J. Am. Chem. Soc. 2015, 137, 8644−8653

■ ACKNOWLEDGMENTS

The authors gratefully acknowledge research support of this work by the French National Agency for Research (no. ANR-09-JCJC-0087), Labex arcane (ANR-11-LABX-003), and COST Action (CM1305 ECOSTBio, Explicit Control Over Spin-States in Technology and Biochemistry). C.J.P., S.D., M.R., D.A.P. and F.N. gratefully acknowledge support from the Max Planck Society. M.V.C. thanks P. Legrand at beamline PROXIMA1 from SOLEIL for help with X-ray data collection. M.R. and R.C .acknowledge the CNRS, the University of Bordeaux, the Aquitaine Région, and the GDR MCM2. Portions of this research were carried out at the Stanford Synchrotron Radiation Lightsource, a national user facility operated by Stanford University on behalf of the U.S. Department of Energy, Office of Basic Energy Sciences.

■ REFERENCES

(1) Simándi, L. I. *Advances in Catalytic Activation of Dioxygen by Metal Complexes*; Catalysis by Metal Complexes *26*; Kluwer Academic Publishers: Dordrecht, 2002.
(2) Arakawa, H.; Aresta, M.; Armor, J. N.; Barteau, M. A.; Beckman, E. J.; Bell, A. T.; Bercaw, J. E.; Creutz, C.; Dinjus, E.; Dixon, D. A.; Domen, K.; DuBois, D. L.; Eckert, J.; Fujita, E.; Gibson, D. H.; Goddard, W. A.; Goodman, D. W.; Keller, J.; Kubas, G. J.; Kung, H. H.; Lyons, J. E.; Manzer, L. E.; Marks, T. J.; Morokuma, K.; Nicholas, K. M.; Periana, R.; Que, L.; Rostrup-Nielson, J.; Sachtler, W. M. H.; Schmidt, L. D.; Sen, A.; Somorjai, G. A.; Stair, P. C.; Stults, B. R.; Tumas, W. *Chem. Rev.* **2001**, *101*, 953.
(3) Shilov, A. E.; Shul'pin, G. B. *Chem. Rev.* **1997**, *97*, 2879.
(4) Ferguson-Miller, S.; Babcock, G. T. *Chem. Rev.* **1996**, *96*, 2889.
(5) Kaila, V. R. I.; Verkhovsky, M. I.; Wikstrom, M. *Chem. Rev.* **2010**, *110*, 7062.
(6) Adler, S. B. *Chem. Rev.* **2004**, *104*, 4791.
(7) Winter, M.; Brodd, R. J. *Chem. Rev.* **2004**, *104*, 4245.
(8) Egami, H.; Oguma, T.; Katsuki, T. *J. Am. Chem. Soc.* **2010**, *132*, 5886.
(9) Hermans, I.; Spier, E. S.; Neuenschwander, U.; Turra, N.; Baiker, A. *Top. Catal.* **2009**, *52*, 1162.
(10) Yamada, Y.; Fukunishi, Y.; Yamazaki, S.-i.; Fukuzumi, S. *Chem. Commun.* **2010**, *46*, 7334.
(11) Mase, K.; Ohkubo, K.; Fukuzumi, S. *Inorg. Chem.* **2015**, *54*, 1808.
(12) Mousavi Shaegh, S. A.; Nguyen, N.-T.; Mousavi Ehteshami, S. M.; Chan, S. H. *Energy Environ. Sci.* **2012**, *5*, 8225.
(13) Yamazaki, S.-i.; Siroma, Z.; Senoh, H.; Ioroi, T.; Fujiwara, N.; Yasuda, K. *J. Power Sources* **2008**, *178*, 20.
(14) Tolman, W. B.; Solomon, E. I. *Inorg. Chem.* **2010**, *49*, 3555.
(15) Ray, K.; Pfaff, F. F.; Wang, B.; Nam, W. *J. Am. Chem. Soc.* **2014**, *136*, 13942.
(16) Fukuzumi, S.; Okamoto, K.; Gros, C. P.; Guilard, R. *J. Am. Chem. Soc.* **2004**, *126*, 10441.
(17) Rosenthal, J.; Nocera, D. G. *Acc. Chem. Res.* **2007**, *40*, 543.
(18) Halime, Z.; Kotani, H.; Li, Y.; Fukuzumi, S.; Karlin, K. D. *Proc. Natl. Acad. Sci. U.S.A.* **2011**, *108*, 13990.
(19) Tahsini, L.; Kotani, H.; Lee, Y.-M.; Cho, J.; Nam, W.; Karlin, K. D.; Fukuzumi, S. *Chem.—Eur. J.* **2012**, *18*, 1084.
(20) Fukuzumi, S.; Mochizuki, S.; Tanaka, T. *J. Chem. Soc., Chem. Commun.* **1989**, 391.
(21) Olaya, A. J.; Schaming, D.; Brevet, P.-F.; Nagatani, H.; Zimmermann, T.; Vanicek, J.; Xu, H.-J.; Gros, C. P.; Barbe, J.-M.; Girault, H. H. *J. Am. Chem. Soc.* **2012**, *134*, 498.
(22) Peljo, P.; Murtomaki, L.; Kallio, T.; Xu, H.-J.; Meyer, M.; Gros, C. P.; Barbe, J.-M.; Girault, H. H.; Laasonen, K.; Kontturi, K. *J. Am. Chem. Soc.* **2012**, *134*, 5974.
(23) Costas, M.; Mehn, M. P.; Jensen, M. P.; Que, L. *Chem. Rev.* **2004**, *104*, 939.
(24) Decker, A.; Solomon, E. I. *Curr. Opin. Chem. Biol.* **2005**, *9*, 152.
(25) Solomon, E. I.; Brunold, T. C.; Davis, M. I.; Kemsley, J. N.; Lee, S. K.; Lehnert, N.; Neese, F.; Skulan, A. J.; Yang, Y. S.; Zhou, J. *Chem. Rev.* **2000**, *100*, 235.
(26) Liu, S.; Mase, K.; Bougher, C.; Hicks, S. D.; Abu-Omar, M. M.; Fukuzumi, S. *Inorg. Chem.* **2014**, *53*, 7780.
(27) Kakuda, S.; Rolle, C. J.; Ohkubo, K.; Siegler, M. A.; Karlin, K. D.; Fukuzumi, S. *J. Am. Chem. Soc.* **2015**, *137*, 3330.
(28) Hamberg, M.; Su, C.; Oliw, E. *J. Biol. Chem.* **1998**, *273*, 13080.
(29) Su, C.; Sahlin, M.; Oliw, E. H. *J. Biol. Chem.* **2000**, *275*, 18830.
(30) Boal, A. K.; Cotruvo, J. A., Jr.; Stubbe, J.; Rosenzweig, A. C. *Science* **2010**, *329*, 1526.
(31) Miller, A.-F. *Curr. Opin. Chem. Biol.* **2004**, *8*, 162.
(32) Wu, J.; Penner-Hahn, J. E.; Pecoraro, V. L. *Chem. Rev.* **2004**, *104*, 903.
(33) Umena, Y.; Kawakami, K.; Shen, J.-R.; Kamiya, N. *Nature* **2011**, *473*, 55.
(34) Mullins, C. S.; Pecoraro, V. L. *Coord. Chem. Rev.* **2008**, *252*, 416.
(35) Pecoraro, V. L.; Baldwin, M. J.; Gelasco, A. *Chem. Rev.* **1994**, *94*, 807.
(36) Signorella, S.; Hureau, C. *Coord. Chem. Rev.* **2012**, *256*, 1229.
(37) Kovacs, J. A.; Brines, L. M. *Acc. Chem. Res.* **2007**, *40*, 501.
(38) Coggins, M. K.; Sun, X.; Kwak, Y.; Solomon, E. I.; Rybak-Akimova, E. V.; Kovacs, J. A. *J. Am. Chem. Soc.* **2013**, *135*, 5631.
(39) Lee, C.-M.; Chuo, C.-H.; Chen, C.-H.; Hu, C.-C.; Chiang, M.-H.; Tseng, Y.-J.; Hu, C.-H.; Lee, G.-H. *Angew. Chem., Int. Ed.* **2012**, *51*, 5427.
(40) Namuswe, F.; Kasper, G. D.; Sarjeant, A. A. N.; Hayashi, T.; Krest, C. M.; Green, M. T.; Moenne-Loccoz, P.; Goldberg, D. P. *J. Am. Chem. Soc.* **2008**, *130*, 14189.
(41) Jiang, Y.; Telser, J.; Goldberg, D. P. *Chem. Commun.* **2009**, 6828.
(42) Coggins, M. K.; Kovacs, J. A. *J. Am. Chem. Soc.* **2011**, *133*, 12470.
(43) Coggins, M. K.; Martin-Diaconescu, V.; DeBeer, S.; Kovacs, J. A. *J. Am. Chem. Soc.* **2013**, *135*, 4260.
(44) Krishnamurthy, D.; Kasper, G. D.; Namuswe, F.; Kerber, W. D.; Narducci Sarjeant, A. A.; Moenne-Loccoz, P.; Goldberg, D. P. *J. Am. Chem. Soc.* **2006**, *128*, 14222.
(45) Brown, C. D.; Neidig, M. L.; Neibergall, M. B.; Lipscomb, J. D.; Solomon, E. I. *J. Am. Chem. Soc.* **2007**, *129*, 7427.
(46) Brines, L. M.; Shearer, J.; Fender, J. K.; Schweitzer, D.; Shoner, S. C.; Barnhart, D.; Kaminsky, W.; Lovell, S.; Kovacs, J. A. *Inorg. Chem.* **2007**, *46*, 9267.
(47) Kitagawa, T.; Dey, A.; Lugo-Mas, P.; Benedict, J. B.; Kaminsky, W.; Solomon, E.; Kovacs, J. A. *J. Am. Chem. Soc.* **2006**, *128*, 14448.
(48) Green, M. T.; Dawson, J. H.; Gray, H. B. *Science* **2004**, *304*, 1653.
(49) Coggins, M. K.; Toledo, S.; Shaffer, E.; Kaminsky, W.; Shearer, J.; Kovacs, J. A. *Inorg. Chem.* **2012**, *51*, 6633.
(50) DuBois, D. L. *Inorg. Chem.* **2014**, *53*, 3935.
(51) Shook, R. L.; Borovik, A. S. *Inorg. Chem.* **2010**, *49*, 3646.
(52) Shook, R. L.; Gunderson, W. A.; Greaves, J.; Ziller, J. W.; Hendrich, M. P.; Borovik, A. S. *J. Am. Chem. Soc.* **2008**, *130*, 8888.
(53) Carver, C. T.; Matson, B. D.; Mayer, J. M. *J. Am. Chem. Soc.* **2012**, *134*, 5444.
(54) Borovik, A. S. *Acc. Chem. Res.* **2005**, *38*, 54.
(55) Kopf, M. A.; Varech, D.; Tuchagues, J. P.; Mansuy, D.; Artaud, I. *J. Chem. Soc., Dalton Trans.* **1998**, 991.
(56) Cheng, B.; Cukiernik, F.; Fries, P. H.; Marchon, J.-C.; Scheidt, W. R. *Inorg. Chem.* **1995**, *34*, 4627.
(57) Cheng, B.; Fries, P. H.; Marchon, J.-C.; Scheidt, W. R. *Inorg. Chem.* **1996**, *35*, 1024.
(58) Biswas, S.; Mitra, K.; Adhikary, B.; Lucas, C. R. *Transition Met. Chem.* **2005**, *30*, 586.
(59) Zhou, H. B.; Wang, H. S.; Chen, Y.; Xu, Y. L.; Song, X. J.; Song, Y.; Zhang, Y. Q.; You, X. Z. *Dalton Trans.* **2011**, *40*, 5999.
(60) Mukhopadhyay, S.; Mandal, S. K.; Bhaduri, S.; Armstrong, W. H. *Chem. Rev.* **2004**, *104*, 3981.

DOI: 10.1021/jacs.5b04917
J. Am. Chem. Soc. 2015, 137, 8644−8653

(61) Visser, H.; Anxolabéhère-Mallart, E.; Bergmann, U.; Glatzel, P.; Robblee, J. H.; Cramer, S. P.; Girerd, J.-J.; Sauer, K.; Klein, M. P.; Yachandra, V. K. *J. Am. Chem. Soc.* **2001**, *123*, 7031.
(62) Roemelt, M.; Beckwith, M. A.; Duboc, C.; Collomb, M. N.; Neese, F.; DeBeer, S. *Inorg. Chem.* **2012**, *51*, 680.
(63) O'Connor, C. J. *Prog. Inorg. Chem.* **1982**, *29*, 203.
(64) Wieghardt, K. *Angew. Chem., Int. Ed. Engl.* **1989**, *28*, 1153.
(65) Blanchard, S.; Blain, G.; Rivière, E.; Nierlich, M.; Blondin, G. *Chem.—Eur. J.* **2003**, *9*, 4260.
(66) Mikuriya, M.; Adachi, F.; Iwasawa, H.; Handa, M.; Koikawa, M.; Okawa, H. *Bull. Chem. Soc. Jpn.* **1994**, *67*, 3263.
(67) Gennari, M.; Pécaut, J.; DeBeer, S.; Neese, F.; Collomb, M.-N.; Duboc, C. *Angew. Chem., Int. Ed.* **2011**, *50*, 5662.
(68) Hillier, W.; Wydrzynski, T. *Coord. Chem. Rev.* **2008**, *252*, 306.
(69) Hillier, W.; Messinger, J.; Wydrzynski, T. *Biochemistry* **1998**, *37*, 16908.
(70) Matsubara, C.; Kawamoto, N.; Takamura, K. *Analyst* **1992**, *117*, 1781.
(71) Takamura, K.; Matsubara, C.; Matsumoto, T. *Anal. Sci.* **2008**, *24*, 401.
(72) Fukuzumi, S.; Kotani, H.; Lucas, H. R.; Doi, K.; Suenobu, T.; Peterson, R. L.; Karlin, K. D. *J. Am. Chem. Soc.* **2010**, *132*, 6874.
(73) Kakuda, S.; Peterson, R. L.; Ohkubo, K.; Karlin, K. D.; Fukuzumi, S. *J. Am. Chem. Soc.* **2013**, *135*, 6513.
(74) Balch, A. L.; Chan, Y. W.; Cheng, R. J.; La Mar, G. N.; Latos-Grazynski, L.; Renner, M. W. *J. Am. Chem. Soc.* **1984**, *106*, 7779.
(75) Coggins, M. K.; Brines, L. M.; Kovacs, J. A. *Inorg. Chem.* **2013**, *52*, 12383.
(76) Root, D. E.; Mahroof-Tahir, M.; Karlin, K. D.; Solomon, E. I. *Inorg. Chem.* **1998**, *37*, 4838.
(77) Chen, P.; Fujisawa, K.; Solomon, E. I. *J. Am. Chem. Soc.* **2000**, *122*, 10177.
(78) Ching, H. Y. V.; Anxolabehere-Mallart, E.; Colmer, H. E.; Costentin, C.; Dorlet, P.; Jackson, T. A.; Policar, C.; Robert, M. *Chem. Sci.* **2014**, *5*, 2304.
(79) Jung, J.; Liu, S.; Ohkubo, K.; Abu-Omar, M. M.; Fukuzumi, S. *Inorg. Chem.* **2015**, *54*, 4285.
(80) Sheriff, T. S. *J. Chem. Soc., Dalton Trans.* **1992**, 1051.
(81) Bettelheim, A.; Ozer, D.; Parash, R. *J. Chem. Soc., Faraday Trans. 1* **1983**, *79*, 1555.

DOI: 10.1021/jacs.5b04917
J. Am. Chem. Soc. 2015, 137, 8644−8653